

# Fusion Product Diagnostics based on Commercially Available Chemical Vapor Deposition Diamond Detector in Large Helical Device

---

**K. Ogawa<sup>a,b,1</sup>, M. Isobe<sup>a,b</sup>, C. Weiss<sup>c,d</sup>, E. Griesmayer<sup>c,d</sup>, S. Sangaroon<sup>e</sup>, E. Takada<sup>f</sup>, S. Masuzaki<sup>a</sup>, H. Ohtani<sup>a,b</sup>, L. Liao<sup>b</sup>, S. Tamaki<sup>g</sup>, I. Murata<sup>g</sup>, and M. Osakabe<sup>a,b</sup>**

<sup>a</sup> National Institute for Fusion Science, National Institutes of Natural Sciences, Toki, 509-5292, Japan

<sup>b</sup> The Graduate University for Advanced Studies, SOKENDAI, Toki, 509-5292, Japan

<sup>c</sup> CIVIDEC Instrumentation GmbH, Schottengasse 3A/1/41, 1010 Wien, Austria

<sup>d</sup> Technischen Universität Wien, Atominstitut, Stadionallee 2, 1020 Wien, Austria

<sup>e</sup> Mahasarakham University, 20 41 Kham Riang, Kantharawichai District, Maha Sarakham 44150, Thailand

<sup>f</sup> National Institute of Technology, Toyama collage, Toyama, 939-8045, Japan

<sup>g</sup> Osaka University, Suita, 565-0871, Japan

E-mail: [ogawa.kunihiro@nifs.ac.jp](mailto:ogawa.kunihiro@nifs.ac.jp)

**ABSTRACT:** Fusion product diagnostics based on four commercially available single-crystal chemical vapor deposition (s-CVD) diamond detectors are installed in the Large Helical Device (LHD) in order to understand energetic ion confinement. Characteristics of s-CVD diamonds were surveyed using alpha and D-T neutron sources. It is found that the energy resolutions of s-CVD diamonds for ~5 MeV alpha particles and 14 MeV neutrons are 1%-3% and ~1.7%, respectively. Moreover, the response of four s-CVD diamond detectors to alpha particles and D-T neutrons is almost identical. The installation positions of the diamond detectors in the vacuum vessel are searched for, based on the loss points of charged fusion products reckoned by Lorentz orbit calculations. Energy- and time-resolved measurement of fusion product flux will progress in further understanding of energetic ion confinement in LHD.

**KEYWORDS:** Diamond Detectors; Neutron detectors; Plasma diagnostics - charged-particle spectroscopy.

---

34	<b>Contents</b>	
35	<b>1. Introduction</b>	<b>1</b>
36	<b>2. Commercially available chemical vapor deposition single crystal diamond detector</b>	
37	<b>response to alpha particles</b>	<b>2</b>
38	<b>3. Commercially available chemical vapor deposition single crystal diamond detector</b>	
39	<b>response to D-T neutrons</b>	<b>6</b>
40	<b>4. Uniformity of s-CVD diamond detector for D-T neutron measurement and applicability</b>	
41	<b>to LHD</b>	<b>10</b>
42	<b>5. Installation of commercially available single crystal chemical vapor deposited diamond</b>	
43	<b>detector for fusion product measurement in Large Helical Device</b>	<b>12</b>
44	<b>5.1 Searching for suitable location for fusion products measurement</b>	<b>12</b>
45	<b>5.2 Design of diamond detector for fusion products</b>	<b>14</b>
46	<b>6. Summary</b>	<b>15</b>
47		
48		
49		

---

## 1. Introduction

Research toward fusion power generation, considered to be unlimited clean energy, has been intensively performed to solve energy problems. A phase of this research is about to enter the nuclear-burning plasma era, as represented by ITER[1]. In the upcoming fusion burning plasma research era, neutron diagnostics is regarded as one of the essential diagnostics[2, 3]. In fusion-burning plasmas, neutron energy reflects fuel ion velocity distributions. Therefore, neutron energy spectrum measurements in thermal plasma can provide the fuel ion temperature[4-6], fuel ratio[7-9], and plasma rotation[10]. Moreover, neutron diagnostics provide information on energetic ion confinement in currently functioning neutral-beam-heated or ion-cyclotron-range-of-frequency-heated plasmas[11, 12].

The diamond detectors[13] have been developed to be utilized in fusion plasma research due to their attractive potential in fusion plasma diagnostics, e.g., compactness and their potential for measurement in high-irradiation and high-temperature conditions[14]. This is feasible due to its relatively wide band gap of 5.5 eV, which is wider than that of silicon 1.14 eV. Fusion plasma diagnostics based on a diamond detector, such as a neutral particle analyzer[15-20], a recoiled proton detector[21, 22], and a deuterium-tritium (D-T) neutron detector[23] based on  $^{12}\text{C}(n,\alpha)^9\text{Be}$  reactions[24] have been developed. To measure the ion temperature of 9 keV through D-T neutron energy spectrum broadening[25], the energy resolution of the detector to the D-T neutron should be less than 4%[26]. Previously, D-T neutron spectrometers based on diamond detectors were developed using natural diamond crystals and an energy resolution of  $\sim 2\%$  was achieved [23, 27-29]. Although diamond detectors based on natural diamonds have been utilized and shown high-energy resolution, they have difficulties of cost, stable availability and uniformity of performance. Subsequently, the artificial synthesis of detector-grade

diamonds due to chemical vapor deposition became possible due to technological innovation[30-32]. By the development of a diamond detector based on single crystal chemical vapor deposition (s-CVD), the energy resolution for D-T neutrons of  $\sim 1\%$  was achieved[33-35]. However, the issues of stable supply, cost, the uniformity of performance and stable availability of the detectors are important, especially in constructing a diamond detector array. The commercialization of diamond detectors is awaited to ensure stable supply and low cost. Recently, a CVD diamond detector became commercially available from CIVIDEC[36]. Therefore, we need to check the uniformity of commercial CVD diamond detector performance. In the Large Helical Device (LHD), plasma experiments using deuterium gas have been done since 2017[37, 38]. These were the first deuterium experiments in large-sized stellarator/helical systems. Therefore, advances in energetic particle confinement were expected[39-41] through the neutron diagnostics[42-50] because neutrons are mainly created by so-called beam-thermal reactions [51]. Energetic particle confinement research, e.g., energetic particle confinement in magnetohydrodynamic quiescent plasmas[52-54], visualization of energetic particle transport[55-60], and demonstration of MeV ion confinement[61, 62], has progressed[63, 64]. Recently the beam ion energy spectrum has been studied using D-D neutron energy spectrometers[65-69]. Understanding of beam ion confinement will progress by measurement of the energy spectrum of charged particles produced by D-D reactions, i.e., tritons, protons, and  $^3\text{He}$ , by D-T reactions, i.e., alpha particles, and by p- $^{11}\text{B}$  reactions, i.e., alpha particles, because their energy has information on beam or MeV ion energies. Also, the D-T neutron energy spectrum can provide information on 1 MeV triton anisotropy. Moreover, understanding a tritium inventory is one of the important tasks[70-72]. An tritium inventory has been mainly compiled, based on annual measurement, using a tritium imaging plate technique[38, 73, 74]. A tritium production rate in each discharge has been evaluated[75] by the CONV\_FIT3D code[76]. A time-resolved measurement of escaping triton flux can make progress in understanding the tritium inventory. This paper describes the performance and reproducibility of commercially available s-CVD diamond detectors and their installation as fusion product diagnostics.

## **2. Commercially available chemical vapor deposition single crystal diamond detector response to alpha particles**

This paper surveyed commercially available s-CVD diamond detectors (B12, CIVIDEC)[77] shown in Fig. 1 a. We obtained the s-CVD diamond detectors' response to alpha particles using an alpha particle calibration source in a laboratory in the LHD building. Figure 1 b and c shows the setup for this calibration. The diamond detector was placed inside the vacuum vessel, and we put the alpha particle calibration source in front of the detector at a distance of 1 mm. The alpha particle calibration source contained  $^{241}\text{Am}$  100 Bq,  $^{244}\text{Cm}$  50 Bq, and  $^{237}\text{Np}$  150 Bq on 20th April 2022. Note that the alpha particle energy of  $^{241}\text{Am}$ ,  $^{244}\text{Cm}$ , and  $^{237}\text{Np}$ , are 5.49 MeV, 5.80 MeV, and 4.96 MeV, respectively. The diamond detector was connected with a charge sensitive preamplifier (Cx-L, CIVIDEC)[78] through an SMA J-J connector. Note that the Cx-L output a semi-Gaussian shape pulse having a width of  $\sim 150$  ns. The pulse width is narrow compared with the pulse width outputted by a conventional shaping amplifier of  $\sim 1$   $\mu\text{s}$  [79]. Therefore, a relatively high-counting rate operation was possible using the Cx-L preamplifier. In addition, the Cx-L can accept a relatively long cable between the diamond detector and preamplifier of up to 1000 pF. The preamplifier signal was transferred to the data acquisition system (DAQ) using a double-shield 15 m 50-Ohm cable (3D-FB). The output signal was

117 acquired by the DAQ, consisting of a 14-bit and up to 500 MHz sampling rate analog to digital  
 118 converter, and a field programmable gate array, providing online and offline pulse shape  
 119 analysis functions (APV8508-14, Techno AP)[80]. Here the charge integral of one pulse  $Q_{\text{total}}$   
 120 was calculated online. The high voltage +360 V, corresponding to 0.72 V/ $\mu\text{m}$ , to the diamond  
 121 detector was applied by a high voltage module (428, ORTEC). The power to the preamplifier  
 122 was provided by a low-voltage-ripple switching power supply (PLD-18-2, Matsusada Precision  
 123 Inc.). The typical pulse count rate obtained in this calibration was 30 counts per second. The  
 124 pileup effect was negligibly small. The  $Q_{\text{total}}$  spectrum obtained by this calibration is shown in  
 125 Fig. 2a. The peaks on  $\sim 4400$ ,  $\sim 5100$ , and  $\sim 5400$  channels correspond to 4.96 MeV, 5.49 MeV,  
 126 and 5.80 MeV, respectively. Figure 2b shows the relation between  $Q_{\text{total}}$  and alpha particle  
 127 energy  $E_{\alpha}$ . The energy calibration of the diamond detector using three peaks was performed  
 128 using the linear function  $E_{\alpha} [\text{keV}] = a \times Q_{\text{total}} + b$ . The coefficient of  $(a, b)$  is (1.155, -1.289),  
 129 (1.179, -1.353), (1.147, -1.301), and (1.167, -1.254) for B120033, B120034, B120035, and  
 130 B120036, respectively. It is worth noting that the difference in the coefficient obtained in four  
 131 different detectors is only 3%. Figure 2c shows the energy resolution (full width at half  
 132 maximum)/(peak position) for each detector for respective  $E_{\alpha}$ . The energy resolution is 1% to  
 133 3%. Here, the energy resolution was relatively lower than the previous report of s-CVD  
 134 diamond detector [81] due to the shorter distance between the alpha source and the diamond  
 135 detector. It was found that the performance of each commercially available s-CVD diamond  
 136 detector was well aligned.

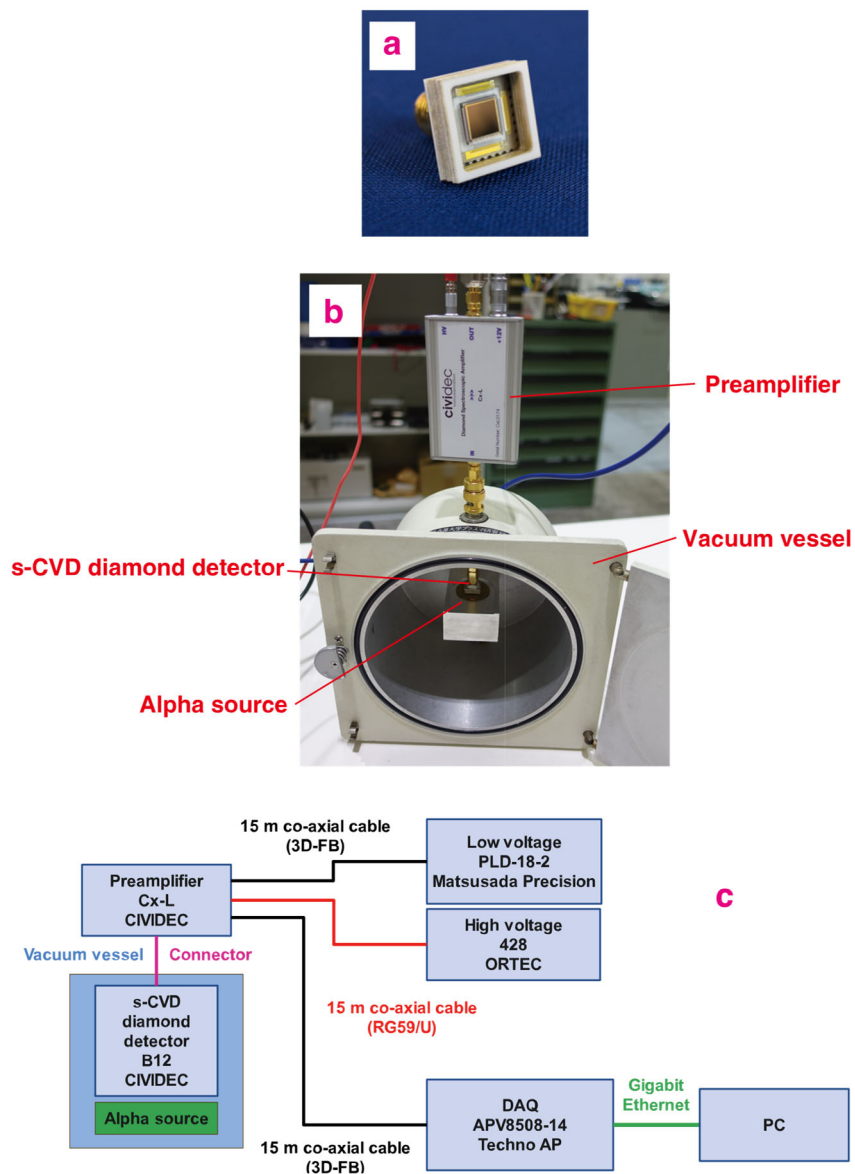


**Figure 1.** a) s-CVD diamond detector B12 b) Experimental setup of s-CVD diamond detector calibration using  $^{241}\text{Am}$ ,  $^{244}\text{Cm}$ , and  $^{237}\text{Np}$  alpha sources. c) Block diagram for alpha calibrations.

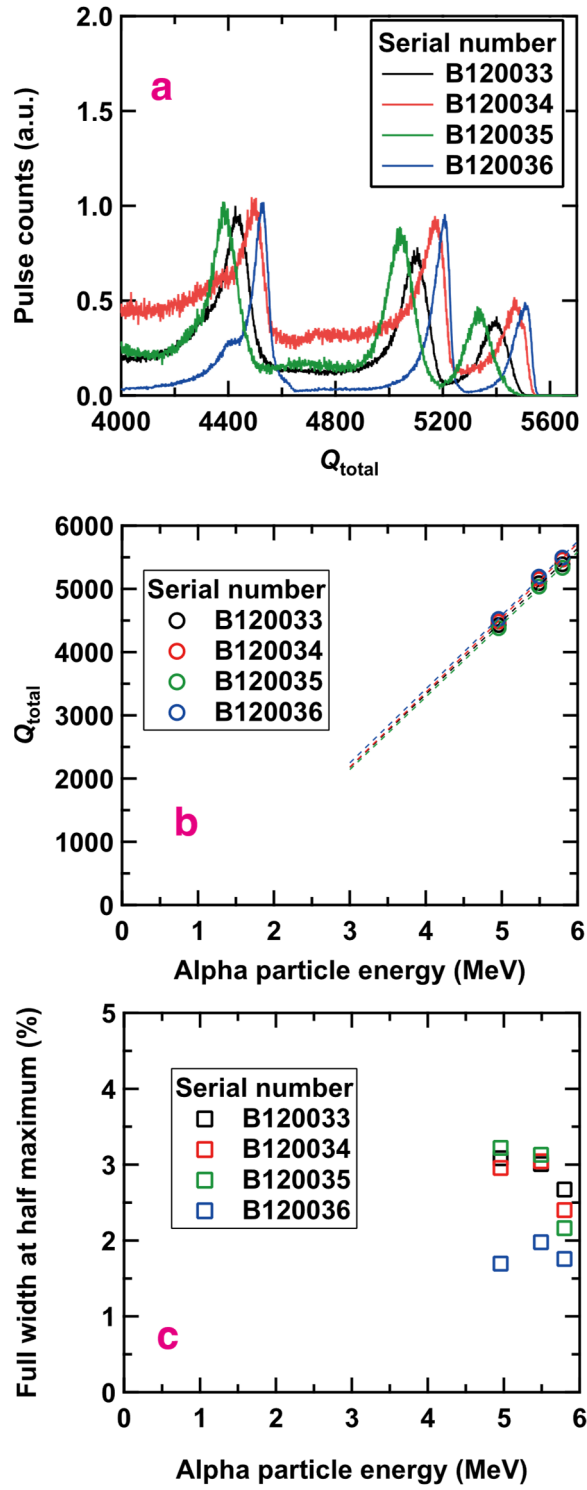


**Figure 2.** a) Charge integral of one pulse ( $Q_{total}$ ) spectrum obtained by four s-CVD diamond detectors in alpha calibration. b) Dependence of  $Q_{total}$  on alpha particle energy. c) Energy resolution of each s-CVD diamond detector for alpha source.

### **3. Commercially available chemical vapor deposition single crystal diamond detector response to D-T neutrons**

The response of s-CVD diamond detectors to D-T neutrons was obtained in the accelerator-based D-T neutron source OKTAVIAN at Osaka University[82]. Figure 3 shows the setups for D-T neutron calibration in OKTAVIAN. A 250 keV/90  $\mu$ A deuteron beam was injected into a 5  $\mu$ m thick tritium-occlusion titanium target. The typical D-T neutron emission rate from the target was  $10^9$  n/s, and the measurement time was set to 15 minutes. The diamond detector was placed at the front or the side of the titanium target. The diamond detector was connected with the charge sensitive preamplifier (Cx-L, CIVIDEC) through the SMA J-J connector. The output signal was transferred to the DAQ (APV8508-14, Techno AP) using a double-shield 15 m 50-Ohm cable (3D-FB). The high voltage +360 V to the diamond detector was applied by the high voltage module (428, ORTEC). The power to the preamplifier was provided by switching power supply (PLD-18-2, Matsusada Precision Inc.). Here, the DAQ, high voltage module, and power supply were located outside a high-intense neutron irradiation room to avoid the irradiation effect[83].

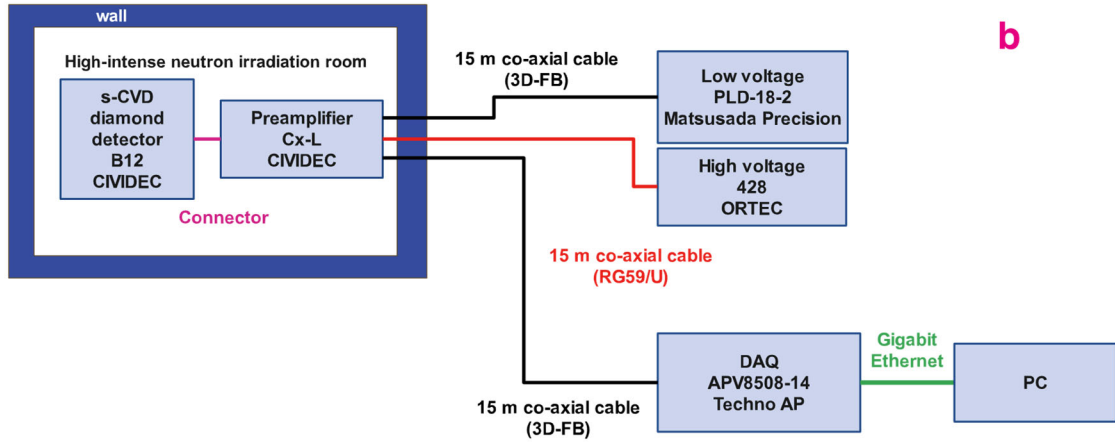


**Figure 3.** a) Experimental setups for D-T neutron measurement using s-CVD diamond detector in OKTAVIAN in Osaka University. b) Block diagram for D-T neutron measurement.

First, the s-CVD diamond detector response to the D-T neutrons was obtained by changing the detector angle with respect to the beam axis at 0, 27, 48, and 81 degrees. The typical pulse counting rate in this experiment was 800 counts per second. Therefore, the pileup effect was negligibly small,  $\sim 0.01\%$ . Figure 4a shows the  $Q_{\text{total}}$  spectra obtained by the diamond detector (B120033). The peak at approximately 7000 channels corresponded to a  $^{12}\text{C}(n,\alpha)^9\text{Be}$  reaction. The position of the  $^{12}\text{C}(n,\alpha)^9\text{Be}$  reaction peak shift and broadness of the peak change depended on the detector angle, due to the D-T neutron spectrum at the detector position. The full width at a half maximum of the  $^{12}\text{C}(n,\alpha)^9\text{Be}$  reaction peaks were 4.6%, 3.8%, 3.1%, and 2.1% in 0-, 27-, 48-, and 81-degree cases, respectively. The main reason for the broadening of the  $Q_{\text{total}}$  peak might have been the broadening of the D-T neutron spectrum caused by the beam deuteron



energy spectrum inside the thick tritium target. To evaluate the energy resolution of the diamond detector, we calculated the neutron spectrum at the detector position, in each case using the following method. Using the TRIM code[84], the deuteron beam energy spectrum was calculated by considering deuterium beam attenuation inside the tritium target. The source D-T neutron spectrum was calculated using the deuteron beam energy spectrum and a D-T fusion cross section[85]. A Monte Carlo N Particle (MCNP6) code [86] was utilized to calculate three-dimensional neutron transport inside a high-intense neutron irradiation room. Figure 4b shows the neutron energy spectrum at the detector position obtained by the calculation. Energy shift and energy broadening of the D-T neutron spectrum were obtained. By comparing the experimentally obtained  $Q_{\text{total}}$  peak width and calculated neutron spectrum peak width at 81 degrees case, the energy resolution of the detector was obtained at 1.7%. The detection efficiency for 14 MeV neutrons was  $6 \times 10^{-4}$  [pulse counts  $\text{cm}^{-2}$ ].

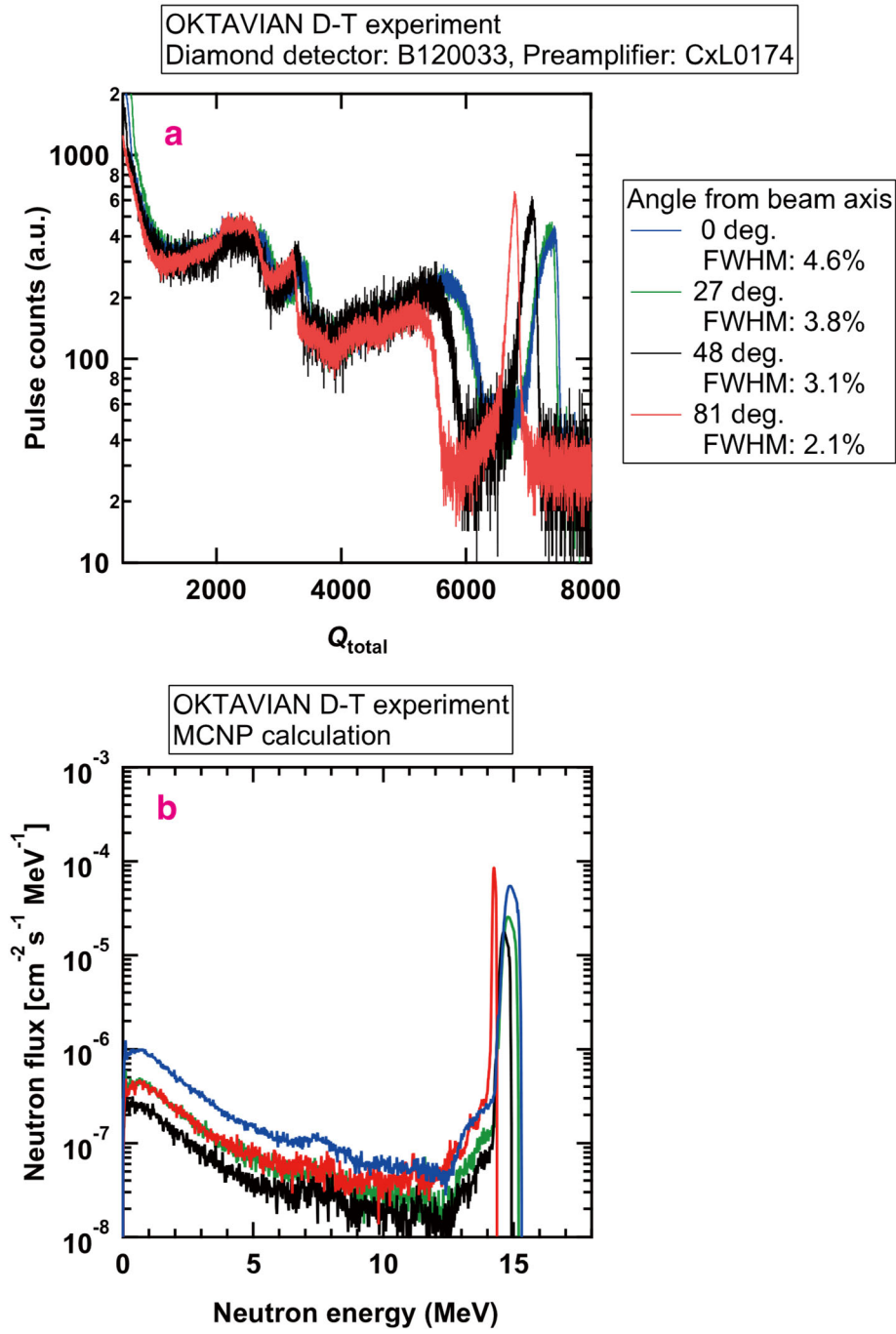


**Figure 4.**a) Charge integral of one pulse ( $Q_{\text{total}}$ ) spectrum obtained by the s-CVD diamond detectors in D-T neutron calibration. Detector angle respects to the beam axis changed from 0 degrees to 81 degrees. b) Neutron flux at the s-CVD diamond detector position in OKTAVIAN calculated by three-dimensional neutron transport calculation MCNP6 code.

#### 4. Uniformity of s-CVD diamond detector for D-T neutron measurement and applicability to LHD

We compared the  $Q_{\text{total}}$  spectrum obtained by the s-CVD diamond detector B12 (B120033) to that obtained by s-CVD diamond detectors (B120034, B120035, and B120036) at 48 degrees (Fig. 5a). The peak due to the  $^{12}\text{C}(n,\alpha)^9\text{Be}$  reaction was located between 6762 to 7316 channels, therefore, the difference was only within 7.5%. These detectors had uniform quality. The diamond detectors had to be located in the vacuum vessel to measure the charged fusion product. Although the B12 can work under ultra-high-vacuum conditions, the preamplifier should be operated outside the vacuum due to outgas and heat removal issues. In the LHD case, the B12 will be placed on the first wall, and the preamplifier will be placed on the diagnostics port. The distance between the B12 and preamplifier positions will be approximately 7 m. Therefore, we checked the signal attenuation and noise level using a 7 m vacuum-tight coaxial cable. Here we used a 50-Ohm ultra-vacuum-tight coaxial cable capable of high-frequency signal measurement (MWX 313, Junkosha)[87]. The capacitance of the 7 m MWX313 cable was 560 pF. The standard insertion loss was 2.9 dB/m for a 1 GHz signal. The pulse height spectra obtained in D-T neutron measurement with and without the 7 m cable are compared in Figure 5b. Even though the pulse height almost halved due to the 7 m cable, the energy resolution degradation was only 0.4%. Note that the signal attenuation might have been due to signal dissipation, due to relatively large capacitance[78].

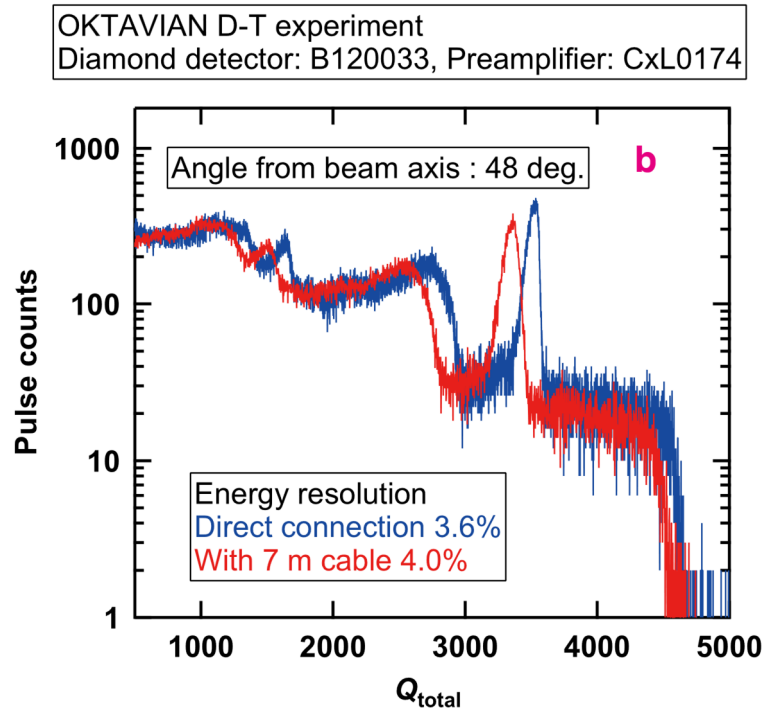
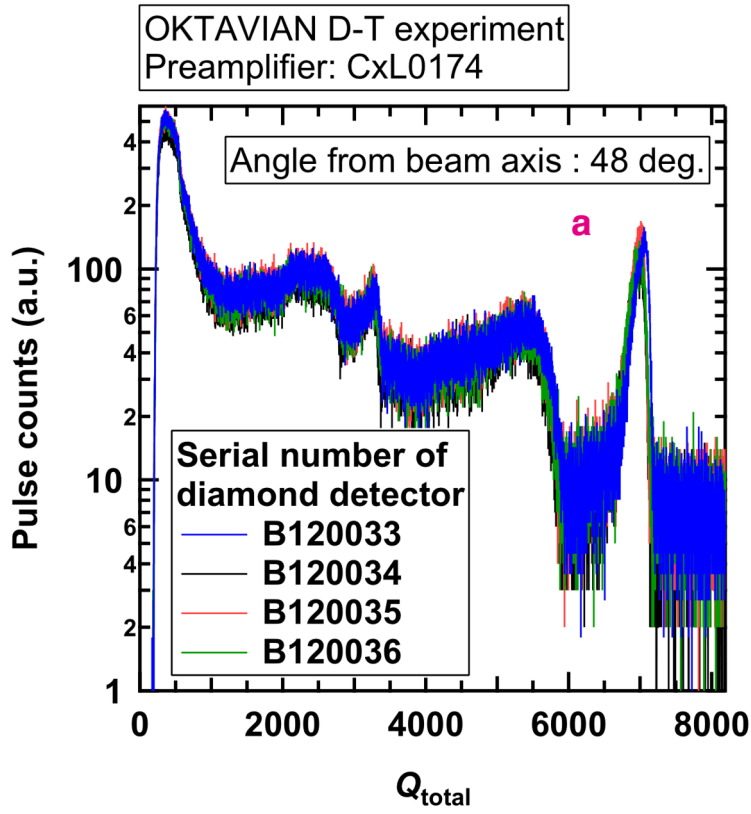


**Figure 5.** Charge integral of one pulse ( $Q_{total}$ ) spectrum obtained by four s-CVD diamond detectors in D-T neutron calibration.  $^{12}\text{C}(n,\alpha)^9\text{Be}$  peak is observed at 7000 channels. The detector angle to the beam axis was 48 degrees. b) Pulse height spectrum obtained with and without 7 m cable between diamond detector and preamplifier. The degradation of energy resolution for  $^{12}\text{C}(n,\alpha)^9\text{Be}$  peak by 7 m cable is only 0.4%.

## **5. Installation of commercially available single crystal chemical vapor deposited diamond detector for fusion product measurement in Large Helical Device**

### **5.1 Searching for suitable location for fusion products measurement**

The location of diamond detectors was decided, based on a collisionless Lorentz orbit following calculation LORBIT,[88] which is widely used in tokamaks[89-92] and stellarators[92-96]. We considered charged fusion products, i.e., D-D fusion born 1 MeV tritons, D-D fusion born 3 MeV protons, D-T fusion born 3.5 MeV alpha particles, and p-<sup>11</sup>B fusion born ~4.0 MeV alpha particles[97]. The magnetic field configuration was chosen to be a toroidal magnetic field strength  $B_t$  of 2.75 T, and the magnetic axis position  $R_{ax}$  of 3.60 m, because approximately 90% of the neutron amount was produced in this configuration[38, 98]. The birth profiles of charged particles were based on the FIT3D-DD code[51, 99, 100], and the birth profile of alpha particles was based on the FBURN code[101]. We launched  $10^7$  particles in each case and saw the loss points of particles on the vacuum vessel and divertor. Figure 6b shows the lost position of particles in 1 MeV tritons with the magnetic field direction from counterclockwise from the top view. Here the lost points appeared on one side of the helical coil due to the gradient  $B$  drift. Figure 6c shows the lost position of particles in 1 MeV tritons with the magnetic field direction of clockwise from the top view. The lost points moved opposite the helical coil side when we changed the magnetic field direction from counterclockwise to clockwise from the top view[102]. We chose four positions suitable for detecting charged fusion products using a virtual reality system[103, 104]. The locations of the detectors ( $x, y, z$ ) were (2507mm, 1900 mm, 1080 mm), (3145 mm, -64 mm, -1080 mm), (2405 mm, 1516 mm, 774 mm), and (2837 mm, 187 mm, -774 mm). Here the original position was set to be the center of the LHD machine, the x-axis set to be 3.5 sections, and the y-axis set to be 1 section of LHD. In addition, we were able to measure 14 MeV neutrons using the  $^{12}\text{C}(n,\alpha)^9\text{Be}$  reaction, using this diamond detector for a triton burnup study in LHD[61]. By estimating a 14 MeV neutron flux using the MCNP6 code [105] considering a maximum triton burnup ratio of 0.45% [62], the expected relative 14 MeV neutron flux in this position was  $10^{-5}$  [ $\text{cm}^{-2}$  per source D-T neutrons][106]. The pulse counting rate in the discharge, with a total neutron rate of  $\sim 10^{15}$  [n/s], which was the typical total neutron rate in deuterium-NB-heated LHD deuterium plasma[63], was expected to be 27 kcps.

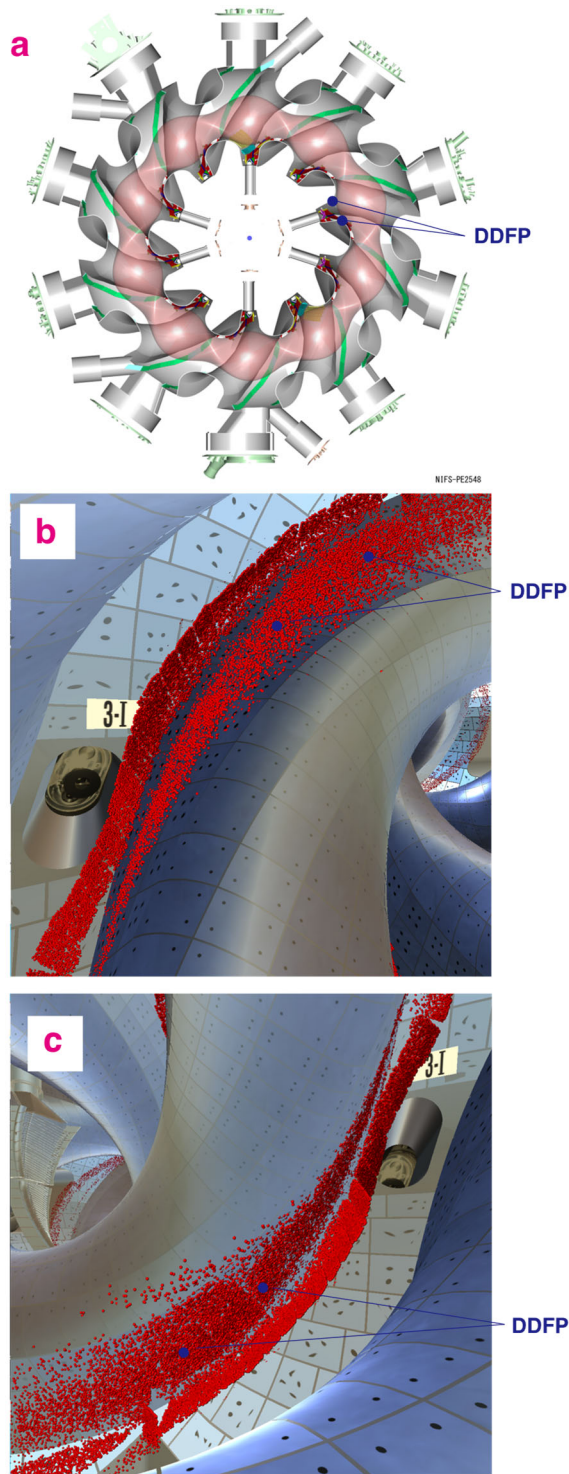


**Figure 6.** a) Bird's eye view of the Large Helical Device and the diamond detector for fusion products (DDFP) position. Loss points of the 1 MeV triton on the first wall and DDFP position in the b) counterclockwise and c) clockwise direction of the toroidal magnetic field from the top view.

## 5.2 Design of diamond detector for fusion products

We installed diamond detectors for fusion products (DDFP) consisting of four-s-CVD detectors in LHD. Fig. 7 shows the setup of the DDFP. The protective tile of the LHD first wall was modified to mount the B12 detector. A thin titanium foil of 2  $\mu\text{m}$  thickness was inserted in the front of B12 detector to prevent the low-energy particles and x-rays from entering. The hollow cylindrical cover with a notch was for avoiding graphite stacking on the B12 detector. The 7 m MWX313 cable covered by an SUS316 flexible tube was used to connect the B12 detector to transfer the signal to the diagnostics port. To avoid electrical noise, the preamplifier Cx-L is directly connected to the SMA feedthrough flange on the diagnostics port. The preamplifier signal is transferred by <50 m double shield 50-Ohm cable to the diagnostic rack on the torus hall. The signal is acquired by a 14-bit 500 MHz sampling ADC (APV8508-14, Techno AP). The  $Q_{\text{total}}$  data of each pulse with the timestamp analyzed online will be stored in the LHD database. An external controllable high voltage module having a logging function applies high voltage (APV3304, Techno AP)[107].

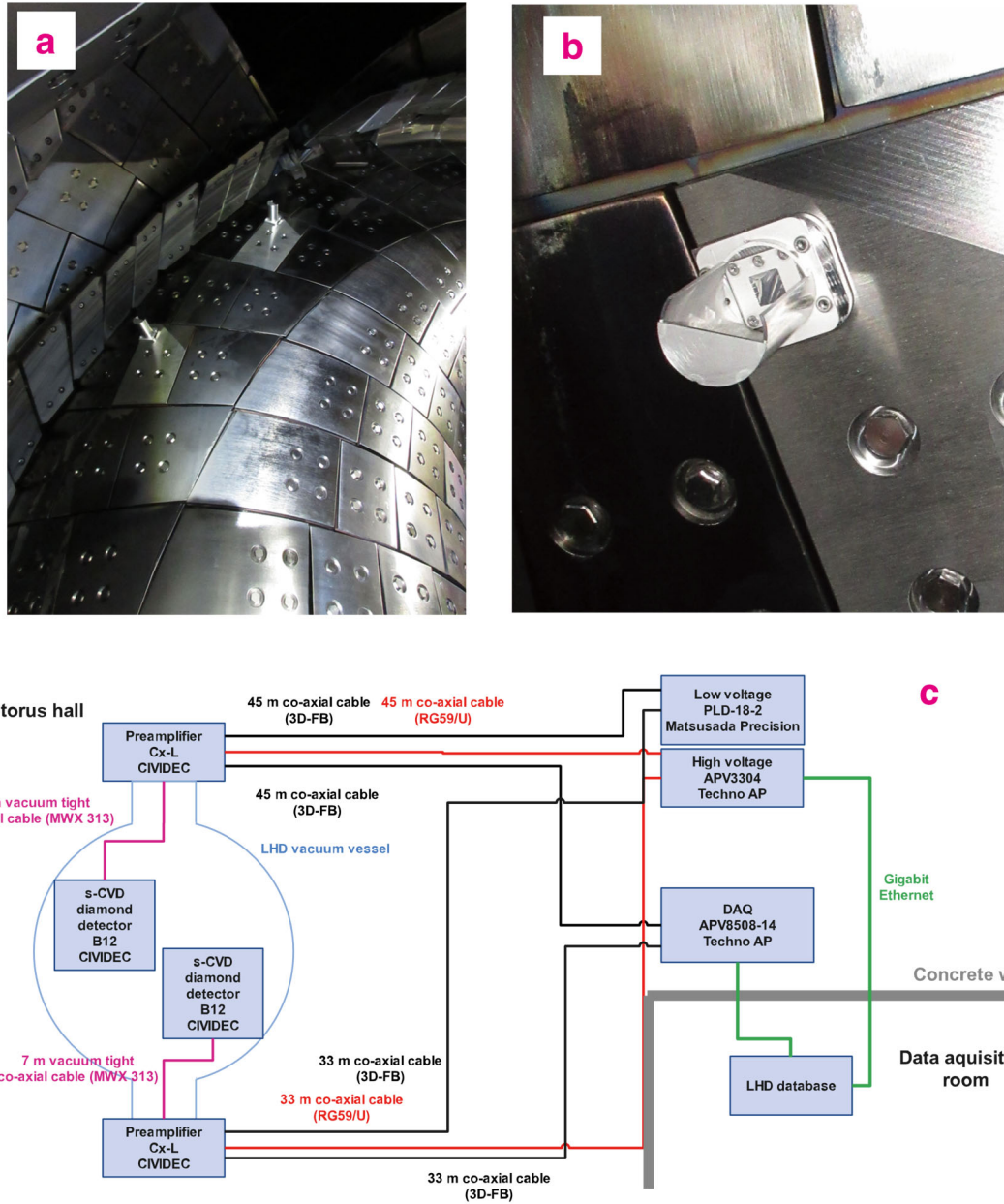


**Figure 7.** a) Diamond detector for fusion product (DDFP) installed in the upper side of LHD and b) zoomed photo. c) Block diagram of data acquisition and control of DDFP installed in LHD.

## 6. Summary

To understand energetic particle confinement in LHD, a diamond detector for fusion products has been installed. First, the performance of commercially available s-CVD diamond detectors and their uniformity were surveyed using alpha particle and D-T neutron sources. The dependence of the total charge in one pulse signal as a function of alpha particle energy shows



that the difference in slope and offset is only 3%. The energy resolution for alpha particle measurement is less than 3%. The results of D-T neutron measurement show the energy resolution for 14 MeV neutrons is 1.7%, which is enough for fuel ion temperature measurement in fusion burning plasmas, and the pulse height spectrum obtained by four detectors is almost identical. A Lorentz orbit calculation plotted with a virtual reality system is capable of choosing the diamond detector positions inside the LHD vacuum vessel. Further progress of energetic ion confinement in LHD by the DDFP is expected.

## Acknowledgments

We are pleased to acknowledge the assistance of the LHD Experiment Group.

## References

- [1] <https://www.iter.org/>
- [2] Wolle B *Tokamak plasma diagnostics based on measured neutron signals* 1999 *Physics Reports-Review Section of Physics Letters* **312** 1
- [3] Krasilnikov A V, Sasao M, Kaschuck Y A, Nishitani T, Batistoni P, Zaveryaev V S, Popovichev S, Iguchi T, Jarvis O N, Källne J, Fiore C L, Roquemore A L, Heidbrink W W, Fisher R, Gorini G, Prosvirin D V, Tsutskikh A Y, Donné A J H, Costley A E and Walker C I *Status of ITER neutron diagnostic development* 2005 *Nuclear Fusion* **45** 1503
- [4] Faust W R and Harris E G *Energy distribution of neutrons produced by a thermonuclear reaction* 1960 *Nuclear Fusion* **1** 62
- [5] Elevant T, Brelén H E, Lindén P G and Scheffel J *Ion Temperature Profile Measurements in ITER by Means of Neutron Spectroscopy* 1997 *Fusion Technology* **32** 304
- [6] Tardocchi M, Gorini G, Henriksson H and Källne J *Ion temperature and plasma rotation profile effects in the neutron emission spectrum* 2004 *Review of Scientific Instruments* **75** 661
- [7] Källne J, Batistoni P and Gorini G *On the possibility of neutron spectrometry for determination of fuel ion densities in DT plasmas* 1991 *Review of Scientific Instruments* **62** 2871
- [8] Hellesen C, Eriksson J, Conroy S, Ericsson G, Skiba M and Weiszflog M *Fuel ion ratio measurements in reactor relevant neutral beam heated fusion plasmas* 2012 *Review of Scientific Instruments* **83** 10D916
- [9] Eriksson B, Conroy S, Ericsson G, Eriksson J, Hjalmarsson A, Ghani Z, Carvalho I S, Jepsu I, Delabie E, Maslov M, Lennholm M, Rimini F and King D *Determining the fuel ion ratio for D(T) and T(D) plasmas at JET using neutron time-of-flight spectrometry* 2022 *Plasma Physics and Controlled Fusion* **64**

- 294 [10] Gorini G, Källne J and Ballabio L *Neutron spectrometry for plasma rotation* 1997  
295 *Review of Scientific Instruments* **68** 561
- 296 [11] Heidbrink W W and Sadler G J *The Behavior of Fast Ions in Tokamak Experiments*  
297 1994 *Nuclear Fusion* **34** 535
- 298 [12] Fasoli A, Gormenzano C, Berk H L, Breizman B, Briguglio S, Darrow D S, Gorelenkov  
299 N, Heidbrink W W, Jaun A, Konovalov S V, Nazikian R, Noterdaeme J M, Sharapov S,  
300 Shinohara K, Testa D, Tobita K, Todo Y, Vlad G and Zonca F *Chapter 5: Physics of*  
301 *energetic ions* 2007 *Nuclear Fusion* **47** S264
- 302 [13] Kozlov S F, Belcarz E, Hage-Ali M, Stuck R and Siffert P *Diamond nuclear radiation*  
303 *detectors* 1974 *Nuclear Instruments and Methods* **117** 277
- 304 [14] Krasilnikov A V 1996: Springer US) pp 435
- 305 [15] Krasilnikov A V, Medley S S, Gorelenkov N N, Budny R V, Darrow D S and  
306 Roquemore A L *Study of acceleration, confinement and sawtooth induced*  
307 *redistribution of fast resonant protons during ICRH in TFTR* 1999 *Nuclear Fusion* **39**  
308 1111
- 309 [16] Isobe M, Sasao M, Iiduka S, Krasilnikov A V, Murakami S, Mutoh T, Osakabe M,  
310 Sudo S, Kawahata K, Ohyabu N and Motojima O *Charge exchange neutral particle*  
311 *analysis with natural diamond detectors on LHD heliotron* 2001 *Review of Scientific*  
312 *Instruments* **72** 611
- 313 [17] Krasilnikov A V, Sasao M, Isobe M, Kumazawa R, Mutoh T, Takeiri Y, Watari T,  
314 Hartman D A, Murakami S, Alekseev A G, Amosov V N, Kaschuck Y A, Portnov D V,  
315 Saito K, Seki T, Kaneko O, Torii Y, Iizuka S, Osakabe M, Goto M, Yamada H,  
316 Narihara K, Ohyabu N, Motojima O and Group t L H D E *Study of acceleration and*  
317 *confinement of high-energy protons during ICRF and NBI heating in LHD using a*  
318 *natural diamond detector* 2002 *Nuclear Fusion* **42** 759
- 319 [18] Saida T, Sasao M, Isobe M and Krasilnikov A V *Charge exchange fast neutral*  
320 *measurement with natural diamond detectors in neon plasma on LHD* 2003 *Review of*  
321 *Scientific Instruments* **74** 1883
- 322 [19] Saida T, Sasao M, Isobe M, Krasilnikov A V, Kumazawa R, Mutoh T, Watari T, Seki T,  
323 Saito K, Murakami S, Matsuoka K and Group L H D E *Study of ripple-trapped proton*  
324 *behaviour in LHD by two line-of-sight measurements of fast neutrals* 2004 *Nuclear*  
325 *Fusion* **44** 488
- 326 [20] Ishikawa M, Nishitani T, Kusama Y, Sukegawa A, Takechi M, Shinohara K,  
327 Krasilnikov A, Kashuck Y, Sasao M, Isobe M, Baba M and Itoga T *Neutron Emission*  
328 *Profile Measurement and Fast Charge Exchange Neutral Particle Flux Measurement*  
329 *for Transport Analysis of Energetic Ions in JT-60U* 2007 *Plasma and Fusion Research*  
330 **2** 019
- 331 [21] Cazzaniga C, Sunden E A, Binda F, Croci G, Ericsson G, Giacomelli L, Gorini G,  
332 Griesmayer E, Grosso G, Kaveney G, Nocente M, Perelli Cippo E, Rebai M, Syme B,  
333 Tardocchi M and Contributors J-E *Single crystal diamond detector measurements of*

334 *deuterium-deuterium and deuterium-tritium neutrons in Joint European Torus fusion*  
335 *plasmas* 2014 *Rev Sci Instrum* **85** 043506

336 [22] Caiffi B, Osipenko M, Ripani M, Pillon M and Taiuti M *Proton Recoil Telescope Based*  
337 *on Diamond Detectors for the Measurement of Fusion Neutrons* 2016 *IEEE*  
338 *Transactions on Nuclear Science* **63** 2409

339 [23] Krasilnikov A V, Azizov E A, Roquemore A L, Khrunov V S and Young K M *TFTR*  
340 *natural diamond detectors based D-T neutron spectrometry system* 1997 *Review of*  
341 *Scientific Instruments* **68** 553

342 [24] Dmitrievich Kovalchuk V, Igorevich Trotsik V and Dmitrievich Kovalchuk V *Diamond*  
343 *detector as a fast neutron spectrometer* 1994 *Nuclear Instruments and Methods in*  
344 *Physics Research Section A: Accelerators, Spectrometers, Detectors and Associated*  
345 *Equipment* **351** 590

346 [25] Brysk H *Fusion neutron energies and spectra* 1973 *Plasma Physics* **15** 611

347 [26] Andersson Sundén E, Ballabio L, Ceconello M, Conroy S, Ericsson G, Johnson M G,  
348 Gorini G, Hellesen C, Ognissanto F, Ronchi E, Sjöstrand H, Tardocchi M and  
349 Weiszflog M *Evaluation of neutron spectrometer techniques for ITER using synthetic*  
350 *data* 2013 *Nuclear Instruments and Methods in Physics Research Section A:*  
351 *Accelerators, Spectrometers, Detectors and Associated Equipment* **701** 62

352 [27] Krasilnikov A V, Azizov E A, Roquemore A L, Khrunov V S and Young K M *TFTR*  
353 *natural diamond detectors based D-T neutron spectrometry system* 1997 *Review of*  
354 *Scientific Instruments* **68** 553

355 [28] Isobe M, Nishitani T, Krasilnikov A V, Kaneko J and Sasao M *First measurements of*  
356 *triton burnup neutron spectra using a natural diamond detector on JT-60U* 1997  
357 *Fusion Engineering and Design* **34-35** 573

358 [29] Krasilnikov A V, Kaneko J, Isobe M, Maekawa F and Nishitani T *Fusion Neutronic*  
359 *Source deuterium-tritium neutron spectrum measurements using natural diamond*  
360 *detectors* 1997 *Review of Scientific Instruments* **68** 1720

361 [30] Bauer C, Baumann I, Colledani C, Conway J, Delpierre P, Djama F, Dulinski W, Fallou  
362 A, Gan K K, Gilmore R S, Grigoriev E, Hallewell G, Han S, Hessing T, Honschied K,  
363 Hrubec J, Husson D, Kagan H, Kania D, Kass R, Kinnison W, Knöpfle K T, Krammer  
364 M, Llewellyn T J, Manfredi P F, Pan L S, Pernegger H, Pernicka M, Plano R, Re V,  
365 Roe S, Rudge A, Schaeffer M, Schnetzer S, Somalwar S, Speziali V, Stone R, Tapper R  
366 J, Tesarek R, Trischuk W, Turchetta R, Thomson G B, Wagner R, Weilhammer P,  
367 White C, Ziock H and Zoeller M *Radiation hardness studies of CVD diamond detectors*  
368 *1995 Nuclear Instruments and Methods in Physics Research Section A: Accelerators,*  
369 *Spectrometers, Detectors and Associated Equipment* **367** 207

370 [31] Angelone M, Lattanzi D, Pillon M, Marinelli M, Milani E, Tucciarone A, Verona-Rinati  
371 G, Popovichev S, Montekali R M, Vincenti M A and Murari A *Development of single*  
372 *crystal diamond neutron detectors and test at JET tokamak* 2008 *Nuclear Instruments*  
373 *and Methods in Physics Research Section A: Accelerators, Spectrometers, Detectors*  
374 *and Associated Equipment* **595** 616

- 375 [32] Kaneko J H, Teraji T, Hirai Y, Shiraishi M, Kawamura S, Yoshizaki S, Ito T, Ochiai K,  
376 Nishitani T and Sawamura T *Response function measurement of layered type CVD*  
377 *single crystal diamond radiation detectors for 14 MeV neutrons* 2004 *Review of*  
378 *Scientific Instruments* **75** 3581
- 379 [33] Shimaoka T, Kaneko J H, Ochiai K, Tsubota M, Shimmyo H, Chayahara A, Umezawa  
380 H, Watanabe H, Shikata S, Isobe M and Osakabe M *A diamond 14 MeV neutron energy*  
381 *spectrometer with high energy resolution* 2016 *Rev Sci Instrum* **87** 023503
- 382 [34] Giacomelli L, Nocente M, Rebai M, Rigamonti D, Milocco A, Tardocchi M, Chen Z J,  
383 Du T F, Fan T S, Hu Z M, Peng X Y, Hjalmarsson A and Gorini G *Neutron emission*  
384 *spectroscopy of DT plasmas at enhanced energy resolution with diamond detectors*  
385 2016 *Review of Scientific Instruments* **87** 11D822
- 386 [35] Rigamonti D, Giacomelli L, Gorini G, Nocente M, Rebai M, Tardocchi M, Angelone M,  
387 Batistoni P, Cufar A, Ghani Z, Jednorog S, Klix A, Laszynska E, Loreti S, Pillon M,  
388 Popovichev S, Roberts N and Thomas D *Neutron spectroscopy measurements of 14*  
389 *MeV neutrons at unprecedented energy resolution and implications for deuterium–*  
390 *tritium fusion plasma diagnostics* 2018 *Measurement Science and Technology* **29**  
391 045502
- 392 [36] <https://cividec.at/>
- 393 [37] Osakabe M, Takeiri Y, Morisaki T, Motojima G, Ogawa K, Isobe M, Tanaka M,  
394 Murakami S, Shimizu A, Nagaoka K, Takahashi H, Nagasaki K, Takahashi H, Fujita T,  
395 Oya Y, Sakamoto M, Ueda Y, Akiyama T, Kasahara H, Sakakibara S, Sakamoto R,  
396 Tokitani M, Yamada H, Yokoyama M, Yoshimura Y and Grp L E *Current Status of*  
397 *Large Helical Device and Its Prospect for Deuterium Experiment* 2017 *Fusion Science*  
398 *and Technology* **72** 199
- 399 [38] Osakabe M, Takahashi H, Yamada H, Tanaka K, Kobayashi T, Ida K, Ohdachi S,  
400 Varela J, Ogawa K, Kobayashi M, Tsumori K, Ikeda K, Masuzaki S, Tanaka M, Nakata  
401 M, Murakami S, Inagaki S, Mukai K, Sakamoto M, Nagasaki K, Suzuki Y, Isobe M,  
402 Morisaki T and Group T L E *Recent results from deuterium experiments on the large*  
403 *helical device and their contribution to fusion reactor development* 2022 *Nuclear*  
404 *Fusion* **62** 042019
- 405 [39] Takeiri Y *The Large Helical Device: Entering Deuterium Experiment Phase Toward*  
406 *Steady-State Helical Fusion Reactor Based on Achievements in Hydrogen Experiment*  
407 *Phase* 2018 *IEEE Transactions on Plasma Science* **46** 2348
- 408 [40] Takeiri Y *Prospect Toward Steady-State Helical Fusion Reactor Based on Progress of*  
409 *LHD Project Entering the Deuterium Experiment Phase* 2018 *IEEE Transactions on*  
410 *Plasma Science* **46** 1141
- 411 [41] Takeiri Y *Advanced Helical Plasma Research towards a Steady-State Fusion Reactor*  
412 *by Deuterium Experiments in Large Helical Device* 2018 *Atoms* **6** 69
- 413 [42] Isobe M, Ogawa K, Nishitani T, Miyake H, Kobuchi T, Pu N, Kawase H, Takada E,  
414 Tanaka T, Li S Y, Yoshihashi S, Uritani A, Jo J, Murakami S, Osakabe M and Grp L E

415 *Neutron Diagnostics in the Large Helical Device* 2018 *IEEE Transactions on Plasma*  
416 *Science* **46** 2050

417 [43] Ito D, Yazawa H, Tomitaka M, Kumagai T, Kono S, Yamauchi M, Misawa T, Kobuchi  
418 T, Hayashi H, Miyake H, Ogawa K, Nishitani T and Isobe M *Development of a Wide*  
419 *Dynamic Range Neutron Flux Measurement Instrument Having Fast Time Response for*  
420 *Fusion Experiments* 2021 *Plasma and Fusion Research* **16** 1405018

421 [44] Ogawa K, Isobe M, Nishitani T and Kobuchi T *The large helical device vertical*  
422 *neutron camera operating in the MHz counting rate range* 2018 *Rev Sci Instrum* **89**  
423 113509

424 [45] Sangaroon S, Ogawa K, Isobe M, Fujiwara Y, Yamaguchi H, Kamio S, Seki R, Nuga H,  
425 Kobayashi M I and Osakabe M *Characterization of the New Vertical Neutron Camera*  
426 *Designed for the Low Neutron Emission Rate Plasma in Large Helical Device* 2021  
427 *Plasma and Fusion Research* **16** 1402039

428 [46] Takada E, Amitani T, Fujisaki A, Ogawa K, Nishitani T, Isobe M, Jo J, Matsuyama S,  
429 Miwa M and Murata I *Design optimization of a fast-neutron detector with scintillating*  
430 *fibers for triton burnup experiments at fusion experimental devices* 2019 *Rev Sci*  
431 *Instrum* **90** 043503

432 [47] Pu N, Nishitani T, Isobe M, Ogawa K, Kawase H, Tanaka T, Li S Y, Yoshihashi S and  
433 Uritani A *In situ calibration of neutron activation system on the large helical device*  
434 2017 *Rev Sci Instrum* **88** 113302

435 [48] Ogawa K, Isobe M, Kawase H and Nishitani T *Neutron Flux Measurement Using a*  
436 *Fast-Neutron Scintillation Detector with High Temporal Resolution on the Large*  
437 *Helical Device* 2018 *Plasma and Fusion Research* **13** 3402068

438 [49] Ogawa K, Isobe M, Nishitani T, Takada E, Kawase H, Amitani T, Pu N, Jo J, Cheon M,  
439 Kim J, Miwa M, Matsuyama S and Murata I *High detection efficiency scintillating fiber*  
440 *detector for time-resolved measurement of triton burnup 14 MeV neutron in deuterium*  
441 *plasma experiment* 2018 *Rev Sci Instrum* **89** 10I101

442 [50] Ogawa K, Isobe M, Sangaroon S, Takada E, Nakada T, Murakami S, Jo J, Zhong G Q,  
443 Zhang Y, Tamaki S and Murata I *Time-resolved secondary triton burnup 14 MeV*  
444 *neutron measurement by a new scintillating fiber detector in middle total neutron*  
445 *emission ranges in deuterium large helical device plasma experiments* 2021 *AAPPS*  
446 *Bulletin* **31**

447 [51] Seki R, Ogawa K, Isobe M, Yokoyama M, Murakami S, Nuga H, Kamio S, Fujiwara Y,  
448 Osakabe M and Group L E *Evaluation of neutron emission rate with FIT3D-DD code in*  
449 *large helical device* 2019 *Plasma and Fusion Research* **14** 3402126

450 [52] Nuga H, Seki R, Ogawa K, Kamio S, Fujiwara Y, Osakabe M, Isobe M, Nishitani T,  
451 Yokoyama M and Group L E *Analysis of energetic particle confinement in LHD using*  
452 *neutron measurement and simulation codes* 2019 *Plasma and Fusion Research* **14**  
453 3402075

- 454 [53] Nuga H, Seki R, Ogawa K, Kamio S, Fujiwara Y, Yamaguchi H, Osakabe M, Isobe M,  
455 Murakami S and Yokoyama M *Analysis of NB Fast-Ion Loss Mechanisms in MHD*  
456 *Quiescent LHD Plasmas* 2021 *Plasma and Fusion Research* **16** 2402052
- 457 [54] Nuga H, Seki R, Ogawa K, Kamio S, Fujiwara Y, Osakabe M, Isobe M, Nishitani T and  
458 Yokoyama M *Studies of the fast ion confinement in the Large Helical Device by using*  
459 *neutron measurement and integrated codes* 2020 *Journal of Plasma Physics* **86**
- 460 [55] Ogawa K, Isobe M, Kawase H, Nishitani T, Seki R, Osakabe M and Grp L E *Effect of*  
461 *the helically-trapped energetic-ion-driven resistive interchange modes on energetic ion*  
462 *confinement in the Large Helical Device* 2018 *Plasma Physics and Controlled Fusion*  
463 **60** 044005
- 464 [56] Ogawa K, Isobe M, Kawase H, Nishitani T, Seki R, Osakabe M and Grp L E  
465 *Observation of enhanced radial transport of energetic ion due to energetic particle*  
466 *mode destabilized by helically-trapped energetic ion in the Large Helical Device* 2018  
467 *Nuclear Fusion* **58** 044001
- 468 [57] Ogawa K, Isobe M, Sugiyama S, Matsuura H, Spong D A, Nuga H, Seki R, Kamio S,  
469 Fujiwara Y, Yamaguchi H, Osakabe M and Grp L E *Energetic particle transport and*  
470 *loss induced by helically-trapped energetic-ion-driven resistive interchange modes in*  
471 *the Large Helical Device* 2020 *Nuclear Fusion* **60** 112011
- 472 [58] Ogawa K, Isobe M, Nuga H, Kamio S, Fujiwara Y, Kobayashi M I, Sangaroon S,  
473 Takada E, Seki R, Yamaguchi H, Murakami S, Jo J and Osakabe M *A study of beam ion*  
474 *and deuterium-deuterium fusion-born triton transports due to energetic particle-driven*  
475 *magnetohydrodynamic instability in the large helical device deuterium plasmas* 2021  
476 *Nuclear Fusion* **61** 096035
- 477 [59] Ogawa K, Isobe M, Sugiyama S, Spong D A, Sangaroon S, Seki R, Nuga H,  
478 Yamaguchi H, Kamio S, Fujiwara Y, Kobayashi M I, Jo J and Osakabe M  
479 *Characteristics of neutron emission profile from neutral beam heated plasmas of the*  
480 *Large Helical Device at various magnetic field strengths* 2021 *Plasma Physics and*  
481 *Controlled Fusion* **63** 065010
- 482 [60] Ogawa K, Isobe M, Kamio S, Nuga H, Seki R, Sangaroon S, Yamaguchi H, Fujiwara Y,  
483 Takada E, Murakami S, Jo J, Takemura Y, Sakai H, Tanaka K, Tokuzawa T, Yasuhara  
484 R and Osakabe M *Studies of energetic particle transport induced by multiple Alfvén*  
485 *eigenmodes using neutron and escaping energetic particle diagnostics in Large Helical*  
486 *Device deuterium plasmas* 2022 *Nuclear Fusion* **62** 112001
- 487 [61] Ogawa K, Isobe M, Nishitani T, Murakami S, Seki R, Nakata M, Takada E, Kawase H,  
488 Pu N and Grp L E *Time-resolved triton burnup measurement using the scintillating*  
489 *fiber detector in the Large Helical Device* 2018 *Nuclear Fusion* **58** 034002
- 490 [62] Ogawa K, Isobe M, Nishitani T, Murakami S, Seki R, Nuga H, Kamio S, Fujiwara Y,  
491 Yamaguchi H, Saito Y, Maeta S, Osakabe M and Grp L E *Energetic ion confinement*  
492 *studies using comprehensive neutron diagnostics in the Large Helical Device* 2019  
493 *Nuclear Fusion* **59** 076017

494 [63] Isobe M, Ogawa K, Nishitani T, Pu N, Kawase H, Seki R, Nuga H, Takada E,  
495 Murakami S, Suzuki Y, Yokoyama M, Osakabe M and Grp L E *Fusion neutron*  
496 *production with deuterium neutral beam injection and enhancement of energetic-*  
497 *particle physics study in the large helical device* 2018 *Nuclear Fusion* **58** 082004

498 [64] Ogawa K, Isobe M and Osakabe M *Progress on Integrated Neutron Diagnostics for*  
499 *Deuterium Plasma Experiments and Energetic Particle Confinement Studies in the*  
500 *Large Helical Device During the Campaigns from FY2017 to FY2019* 2021 *Plasma and*  
501 *Fusion Research* **16** 1102023

502 [65] Isobe M, Ogawa K, Sangaroon S, Kamio S, Fujiwara Y and Osakabe M *Recent*  
503 *development of neutron and energetic-particle diagnostics for LHD deuterium*  
504 *discharges* 2022 *Journal of Instrumentation* **17** C03036

505 [66] Sangaroon S, Ogawa K and Isobe M *Initial operation of perpendicular line-of-sight*  
506 *compact neutron emission spectrometer in the large helical device* 2022 *Review of*  
507 *Scientific Instruments* **93** 093504

508 [67] Sangaroon S, Ogawa K, Isobe M, Kobayashi M I, Fujiwara Y, Kamio S, Yamaguchi H,  
509 Seki R, Nuga H, Toyama S, Miwa M, Matsuyama S, Takada E, Murakami S, Zhong G  
510 Q and Osakabe M *Neutron energy spectrum measurement using CLYC7-based compact*  
511 *neutron emission spectrometer in the Large Helical Device* 2021 *Journal of*  
512 *Instrumentation* **16** C12025

513 [68] Zhang Y, Ge L, Hu Z, Sun J, Li X, Ogawa K, Isobe M, Sangaroon S, Liao L, Yang D,  
514 Gorini G, Nocente M, Tardocchi M and Fan T *Design and optimization of an advanced*  
515 *time-of-flight neutron spectrometer for deuterium plasmas of the large helical device*  
516 2021 *Review of Scientific Instruments* **92** 053547

517 [69] Sangaroon S, Ogawa K, Isobe M, Kobayashi M I, Fujiwara Y, Kamio S, Yamaguchi H,  
518 Seki R, Nuga H, Takada E, Murakami S, Zhong G Q and Osakabe M *Observation of*  
519 *significant Doppler shift in deuterium-deuterium neutron energy caused by neutral*  
520 *beam injection in the large helical device* 2022 *AAPPS Bulletin* **32** 5

521 [70] Tanaka M, Suzuki N and Kato H *Exhaust behavior of tritium from the large helical*  
522 *device in the first deuterium plasma experiment* 2020 *Journal of Nuclear Science and*  
523 *Technology* **57** 1297

524 [71] Tanaka M, Kato H, Suzuki N, Masuzaki S, Yajima M, Nakada M and Iwata C *Tritium*  
525 *Balance in Large Helical Device during and after the First Deuterium Plasma*  
526 *Experiment Campaign* 2020 *Plasma and Fusion Research* **15** 1405062

527 [72] Tanaka M, Suzuki N, Kato H and Chimura H *Estimation of tritium inventory in exhaust*  
528 *detritiation system for fusion test device in the initial tritium recovery operation* 2021  
529 *Fusion Engineering and Design* **172**

530 [73] Masuzaki S, Otsuka T, Ogawa K, Yajima M, Tokitani M, Zhou Q, Isobe M, Oya Y,  
531 Yoshida N and Nobuta Y *Investigation of remaining tritium in the LHD vacuum vessel*  
532 *after the first deuterium experimental campaign* 2020 *Physica Scripta* **T171** 014068

533 [74] Masuzaki S, Yajima M, Ogawa K, Motojima G, Tanaka M, Tokitani M, Isobe M and  
534 Otsuka T *Investigation of the distribution of remaining tritium in divertor in LHD* 2021  
535 *Nuclear Materials and Energy* **26**

536 [75] Nuga H, Seki R, Ogawa K, Kamio S, Fujiwara Y, Yamaguchi H, Osakabe M, Isobe M  
537 and Yokoyama M *Estimation of the Tritium Yields in Deuterium Fusion Plasmas*  
538 *Considering the Fast-Ion Velocity Distribution Function* 2022 *Plasma and Fusion*  
539 *Research* **17** 2402023

540 [76] Nuga H, Seki R, Ogawa K, Kamio S, Fujiwara Y, Osakabe M, Isobe M, Nishitani T and  
541 Yokoyama M *Analysis of Energetic Particle Confinement in LHD Using Neutron*  
542 *Measurement and Simulation Codes* 2019 *Plasma and Fusion Research* **14** 3402075

543 [77] <https://cividec.at/detectors-B12.html>

544 [78] <https://cividec.at/electronics-Cx-L.html>

545 [79] <https://www.ortec-online.com/products/electronics/amplifiers/572a>

546 [80] <http://www.techno-ap.com/img/APV8508.pdf>

547 [81] Pillon M, Angelone M, Krása A, Plompen A J M, Schillebeeckx P and Sergi M L  
548 *Experimental response functions of a single-crystal diamond detector for 5–20.5MeV*  
549 *neutrons* 2011 *Nuclear Instruments and Methods in Physics Research Section A:*  
550 *Accelerators, Spectrometers, Detectors and Associated Equipment* **640** 185

551 [82] Murata I *IAEA-TECDOC-1743 Compendium of Neutron Beam Facilities for High*  
552 *Precision Nuclear Data Measurements (Vienna: IAEA)* 2014 18

553 [83] Ogawa K, Nishitani T, Isobe M, Murata I, Hatano Y, Matsuyama S, Nakanishi H,  
554 Mukai K, Sato M, Yokota M, Kobuchi T, Nishimura T and Osakabe M *Investigation of*  
555 *irradiation effects on highly integrated leading-edge electronic components of*  
556 *diagnostics and control systems for LHD deuterium operation* 2017 *Nuclear Fusion* **57**  
557 086012

558 [84] <http://www.srim.org/>

559 [85] <https://www-nds.iaea.org/fendl/>

560 [86] Werner C J, Bull J S, Solomon C J, Brown F B, McKinney G W, Rising M E, Dixon D  
561 A, Martz R L, Hughes H G, Cox L J, Zukaitis A J, Armstrong J C, Forster R A and  
562 Casswell L <*Werner-2018-Mcnp-version--release-notes.pdf*> 2018

563 [87] [https://www.gapwireless.com/wp-content/uploads/003\\_mwx3.pdf](https://www.gapwireless.com/wp-content/uploads/003_mwx3.pdf)

564 [88] Isobe M, Funaki D and Sasao M *Lorentz Alpha Orbit Calculation in Search of Position*  
565 *Suitable for Escaping Alpha Particle Diagnostics in ITER* 2009 *Journal of Plasma and Fusion*  
566 *Research* **8** 330

567 [89] Kim J Y, Rhee T, Kim J, Yoon S W, Park B H, Isobe M, Ogawa K and Ko W H *Prompt*  
568 *loss of beam ions in KSTAR plasmas* 2016 *AIP Advances* **6** 105013



- 569 [90] Ogawa K, Zhong G, Zhou R, Li K, Isobe M and Hu L *1 MeV Triton Orbit Analysis in*  
570 *EAST Plasmas 2020 Plasma and Fusion Research* **15** 2402022
- 571 [91] Paenthong W, Wisitsorasak A, Sangaroon S, Prompting J, Ogawa K and Isobe M *Fast-*  
572 *ion orbit analysis in Thailand Tokamak-I 2022 Fusion Engineering and Design* **183**  
573 113254
- 574 [92] Ogawa K, Zhang Y, Zhang J, Sangaroon S, Isobe M and Liu Y *Predictive analysis for*  
575 *triton burnup ratio in HL-2A and HL-2M plasmas 2021 Plasma Physics and Controlled*  
576 *Fusion* **63** 045013
- 577 [93] Ogawa K, Yamamoto S, Sano T, Nakayama Y, Isobe M and Darrow D S *Design of Lost*  
578 *Fast-Ion Probe Based on Thin Faraday Films in Heliotron J 2013 Plasma and Fusion*  
579 *Research* **8** 2402128
- 580 [94] Ogawa K, Bozhnikov S A, Äkäslompolo S, Killer C, Grulke O, Nicolai D,  
581 Satheeswaran G, Isobe M, Osakabe M, Yokoyama M and Wolf R C *Energy-and-pitch-*  
582 *angle-resolved escaping beam ion measurements by Faraday-cup-based fast-ion loss*  
583 *detector in Wendelstein 7-X 2019 Journal of Instrumentation* **14** C09021
- 584 [95] Ogawa K, Isobe M, Seki R, Nuga H, Yamaguchi H, Sangaroon S, Shimizu A, Okamura  
585 S, Takahashi H, Oishi T, Kinoshita S, Murase T, Nakagawa S, Tanoue H, Osakabe M,  
586 Liu H F and Xu Y *Feasibility study of fast ion loss diagnostics for CFQS by beam ion*  
587 *loss calculation on vacuum vessel 2021 Journal of Instrumentation* **16** C09029
- 588 [96] Ogawa K, Isobe M, Nuga H, Seki R, Ohdachi S and Osakabe M *Evaluation of Alpha*  
589 *Particle Emission Rate Due to the  $p$ -(11B) Fusion Reaction in the Large Helical Device*  
590 *2022 Fusion Science and Technology* **78** 175
- 591 [97] Laursen K L, Fynbo H O U, Howard A M and Kirsebom O S *Complete kinematics*  
592 *study of the  $p + 11B \rightarrow 12C$  reaction 2014 Journal of Physics: Conference Series* **569**
- 593 [98] Masuzaki S, Otsuka T, Ogawa K, Yajima M, Tokitani M, Zhou Q, Isobe M, Oya Y,  
594 Yoshida N, Nobuta Y and Grp L E *Investigation of remaining tritium in the LHD*  
595 *vacuum vessel after the first deuterium experimental campaign 2020 Physica Scripta*  
596 **T171** 014068
- 597 [99] Murakami S, Nakajima N and Okamoto M *Finite  $\beta$  Effects on the ICRF and NBI*  
598 *Heating in the Large Helical Device 1995 Fusion Technology* **27** 256
- 599 [100] Vincenzi P, Bolzonella T, Murakami S, Osakabe M, Seki R and Yokoyama M  
600 *Upgrades and application of FIT3D NBI-plasma interaction code in view of LHD*  
601 *deuterium campaigns 2016 Plasma Physics and Controlled Fusion* **58** 125008
- 602 [101] Ogawa K, Isobe M, Nishitani T, Seki R, Nuga H, Murakami S, Nakata M, Pu N,  
603 Osakabe M, Jo J, Cheon M, Kim J, Zhong G Q, Xiao M, Hu L Q and Grp L E *Time*  
604 *dependent neutron emission rate analysis for neutral-beam-heated deuterium plasmas*  
605 *in a helical system and tokamaks 2018 Plasma Physics and Controlled Fusion* **60**  
606 095010

- 607 [102] Ogawa K, Isobe M, Nishitani T, Murakami S, Seki R, Nuga H, Pu N, Osakabe M and  
608 Grp L E *Study of first orbit losses of 1 MeV tritons using the Lorentz orbit code in the*  
609 *LHD* 2019 *Plasma Sci Technol* **21** 025102
- 610 [103] Ohtani H, Ohno N, Mizuguchi N, Shoji M and Ishiguro S *Simulation Data Analysis by*  
611 *Virtual Reality System* 2010 *Plasma and Fusion Research* **5** S2109
- 612 [104] Ohtani H, Masuzaki S, Ogawa K and Ishiguro S *Virtual-reality visualization of loss*  
613 *points of 1 MeV tritons in the Large Helical Device, LHD* 2022 *Journal of Visualization*  
614 **25** 281
- 615 [105] Nishitani T, Ogawa K, Nishimura K and Isobe M *Radiation field estimation for the*  
616 *diagnostic and control components by Monte Carlo neutronics calculations with LHD*  
617 *3-dimensional modeling* 2016 *Plasma and Fusion Research* **11** 2405057
- 618 [106] Nishitani T, Ogawa K and Isobe M *Monte Carlo simulation of the neutron*  
619 *measurement for the Large Helical Device deuterium experiments* 2017 *Fusion*  
620 *Engineering and Design* **123** 1020
- 621 [107] <http://www.techno-ap.com/img/APV3304.pdf>  
622